Fuel 262 (2020) 116506

Contents lists available at ScienceDirect

Fuel

journal homepage: www.elsevier.com/locate/fuel

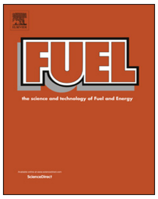

Full Length Article

Modeling the heterogeneous oxidation of elemental mercury by chlorine in flue gas

Fengyang Wang[a,b,1], Guoliang Li[a,b,1], Shuxiao Wang[a,b,*], Qingru Wu[a,b], Lei Zhang[a,b]

[a] *State Key Joint Laboratory of Environment Simulation and Pollution Control, School of Environment, Tsinghua University, Beijing 100084, China*
[b] *State Environmental Protection Key Laboratory of Sources and Control of Air Pollution Complex, Beijing 100084, China*

ARTICLE INFO

Keywords:
Elemental mercury oxidation
Cl addition
Kinetic model

ABSTRACT

The chloride (Cl) addition is an effective mercury oxidation technology. However, it is difficult to determine the optimal amount of Cl addition due to the unanswered question of how elemental mercury (Hg^0) is oxidized by Cl. This study used the one-dimensional drop furnace and heterogeneous oxidation models to study the reaction mechanism between Hg^0 and Cl in the combustion flue gas. This study finds that the Cl and Hg^0 oxidation mechanism follows the E-R mechanism. The formed active Cl atom (Cl*) on the active sites directly oxidizes the Hg^0 into the Hg_2Cl_2 or $HgCl_2$. Then the Hg_2Cl_2 or $HgCl_2$ transfer from active sites into the gas phase. However, when the addition amount exceeds optimum point, the subsequent Cl addition will not further increase the oxidation ratio of Hg^0. The optimum point of Cl addition is 40 ppm via solution impregnation addition but it is 400 ppm via HCl gas addition, respectively. Therefore, the solution impregnation is a more effective method to oxidize Hg^0 compared with the HCl addition in flue gas. These results provide important guidance on the Cl addition practice in the combustion flue gas.

1. Introduction

Coal combustion is one of the main anthropogenic atmosphere mercury emission sources [1–3]. Mercury in the coal is released to the flue gas in the main form of elemental mercury (Hg^0) during the fire processing. Then, the Hg^0 is oxidized when the flue gas temperature decreases from 800 K to 600 K, which determines the mercury speciation ratio in the flue gas before air pollution control devices (APCDs) [4–6]. The Hg^0 was difficult to capture while the oxidization state mercury (Hg^{2+}) and particle mercury (Hg_p) was easy to remove via the wet flue gas desulfurization and dedust equipments [–11]. Therefore, the mercury speciation in the flue gas serving as a significant factor impacts the mercury control effect of APCDs [12]. Catalysis oxidation technology is proven to be a effective Hg^0 oxidation method, but the catalysis activity of catalysts is seriously suppressed via the NH_3 and SO_2 [13,14]. The adsorption technology is a mature mercury capture technology, yet the high price of mercury adsorbent limits the application of mercury adsorption technology [15]. The oxidizing reagents addition was a highly effective and low-cost mercury oxidation technology [16,17]. The halogen addition as an effective method was recommended to transform Hg^0 into oxidization state mercury (Hg^{2+}) with no need for extra equipment addition [18]. T.K. Gale and S.A. Benson et al. systematically researched the influence of halogen addition on the mercury oxidation ratio of coal-fired flue gas in large scale. However, neither of them focused on the mercury and Cl reaction mechanism. Therefore, the reaction mechanism and optimum Cl addition amount was still unambiguous [19,20].

Thermodynamic calculation model, quantum computation theory and dynamic calculation model model have been used to fitting the result of Hg^0 and Cl reaction, but the fitting result could not well reveal the reaction rule [4–6,21–23]. According to previous study, the results of Hg^0 and Cl reaction experiments possibly conformed to the homogeneous and heterogeneous oxidation kinetic models [8,19,20,24,25]. The homogeneous fitting result found that homogeneous models could only partly match the practical data and the homogeneous oxidation kinetic model possibly cannot well fit the mercury oxidation process in flue gas [10,26]. This is attributed to the neglection of heterogeneous oxidation on the surface of fly ash [27–31]. Dunham et al. used 16 fly ash samples to evaluate the mercury oxidation property [27]. The result found that the specific surface area was positive relative with the mercury oxidation ratio, indicating the fly ash played key role on the mercury formation transformation. Therefore, the heterogeneous

---

* Corresponding author at: State Key Joint Laboratory of Environment Simulation and Pollution Control, School of Environment, Tsinghua University, Beijing 100084, China.

E-mail address: shxwang@tsinghua.edu.cn (S. Wang).

[1] These authors contributed equally to this work and should be considered as co-first authors.

https://doi.org/10.1016/j.fuel.2019.116506
Received 28 July 2019; Received in revised form 3 October 2019; Accepted 24 October 2019

oxidation model was possibly more suited to the mercury oxidation mechanism via the Cl.

Langmuir-Hinshelwood (L-H) and Eley-Rideal (E-R) mechanism are the main reaction mechanism of heterogeneous oxidation model. Galbreath et al. and Fujiwara et al. found that the HCl addition promoted the mercury and Cl adsorption on the fly ash [19,20]. This result suggested that mercury oxidation possibly followed the L-H mechanism in flue gas. However, Gale's study found that the HCl adsorbed on the fly ash directly oxidized gaseous mercury [32], indicating the oxidation mechanism conformed to E-R mechanism. The mercury oxidation mechanism is still not clear at present. Moreover, foregoing conclusion was only the inference based on the data came from the fixed bed experiments, which is different from the practical flue gas. As reaction time went on, the active sites of fly ash were gradually occupied via the mercury. The aged fly ash on the fixed bed could not represent the property of new fly ash, possibly resulting in incorrect conclusion. The heterogeneous dynamic reaction models were necessary to be applied to fitting the mercury oxidation processing in real coal-fired flue gas.

Given the lack of present data, this study used the one-dimensional drop furnace to generate coal-fired flue gas, which was in more aligned with actual flue gas. The Cl was added into the flue gas in the form of HCl gas or impregnated into the combusted coal by using $CaCl_2$ and NaCl solution. The different addition concentration was used to explore the effect on the mercury oxidation efficiency and select the optimum addition concentration. The subbituminous coal and lignite coal served as the research fuel. The heterogeneous dynamic models of L-H and E-R mechanism were applied to fitting the experiment result. The mercury oxidation mechanism was investigated via combining the experimental data and theoretical simulation calculation.

2. Material and methods

2.1. Experimental setup and method

The schematic diagram of experiment equipment is shown in Fig. 1. The experiment equipment contains the one-dimensional drop furnace and mercury online monitoring system (Thermo Fisher, 80i, USA). The one-dimensional drop furnace contains coal feeder system, combustion system, air distribution system and monitoring system. The coal fine was carried via the 2.5 L·min^{-1} air at the rate of 20 g·h^{-1}. The coal fine was mixed with the 7.5 L·min^{-1} diluent air and then fed to the drop furnace. The coal fine was combusted at 1100 °C drop furnace. The fly ash in combustion flue gas was collected at ash collector. The flue gas entered into the 6 testing ports. The temperature of 6 testing ports (0–5) decreased from 373 °C to 165 °C. The temperature and residence time of different ports was used to fitting temperature decrease curve. The mercury concentration of testing ports was online measured by a Mercury Freedom™ system (Thermo Fisher Scientific Inc.), which could monitor the concentrations of different gaseous mercury forms, including gaseous elemental mercury (Hg^0), gaseous oxidized mercury (Hg^{2+}) and gaseous total mercury (Hg^t).

$$R_{\mathrm{oxy}} = \frac{Hg^{2+}_{\mathrm{out}}}{Hg^{\mathrm{t}}} \tag{2-1}$$

where the R_{oxi} represents the mercury oxidation ratio; Hg_{out}^{2+} represents the gaseous oxidized mercury in outlet of the reactor. Hg^t represents the gaseous total mercury in testing ports. For the experimental error is inevitable, the Hg^0 removal efficiency is the average of three parallel experimental data and the relative error of all parallel experimental data is less than 10%.

2.2. Coal pretreatment

The lignite (sample 01) from Shanxi and subbituminous coal (sample 02) from Inner Mongolia were used as the researched coals. As shown in Table S1, the content of important elements (Hg, S and Cl) and fly ash was analyzed and contrasted. The S content of subbituminous is far higher than that of the lignite. In the combustion processing, the S element was transformed into SO_2 which played negative role on the mercury oxidation [33,34]. The content of Cl and fly

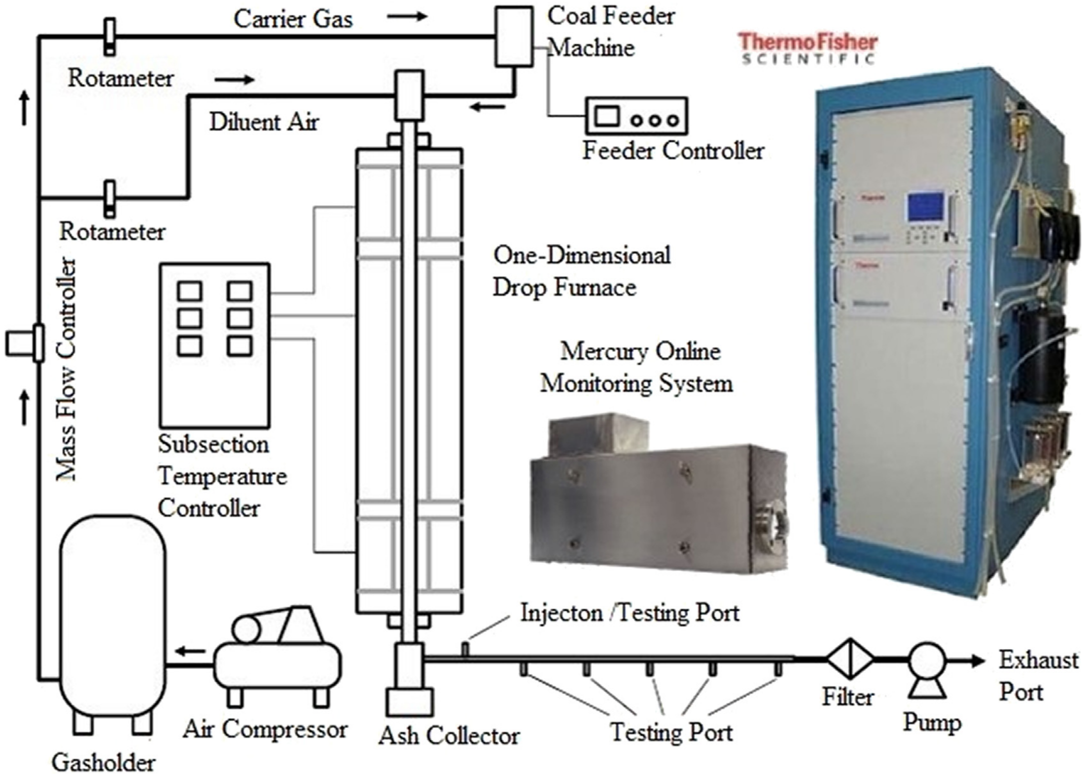

Fig. 1. The schematic diagram of the experiment equipment.

Table 1
The Cl impregnation parameters.

Addition Cl Content (mg·kg^{-1})	Cl Content (mg)	NaCl Solution (g·L^{-1})	NaCl Solution Volume (mL)	$CaCl_2$ Solution (g·L^{-1})	$CaCl_2$ Solution Volume (mL)
100	4.5	2	3.71	1	7.04
300	13.5	2	11.12	1	21.11
500	22.5	2	18.54	5	7.04
700	31.5	5	10.38	5	9.85
1000	45	5	14.83	5	14.07
2000	90	10	14.83	5	28.14
3000	135	10	22.25	15	14.07
5000	225	30	12.36	30	11.73
7500	337.5	30	18.54	30	17.59
10,000	450	30	24.72	30	23.45

Note: the coal mass of data in Table 1 is 45 g.

Table 2
The HCl addition parameter in one-dimensional drop furnace.

The HCl Concentration of Flue Gas (ppm)	Concentration of Addition Gas (ppm)	Addition Flow Rate Gas (L·min^{-1})
15	10,000	0.015
30	10,000	0.030
75	10,000	0.076
150	10,000	0.152
250	10,000	0.256
400	10,000	0.417
600	10,000	0.638
800	20,000	0.416
1000	20,000	0.527

Note: The flow rate of data in Table 2 is 10 L·min^{-1}.

ash is similar. The Chlorine content of lignite and subbituminous coal was 90 and 80 mg·kg^{-1}, respectively. Since the Cl content of two Chinese coal was low and similar, the methods of solution impregnation and HCl gas addition were used to form different concentration flue gases. As shown in Table 1, the Cl content was added from 100 to 10000 mg·kg^{-1} via adjusting the impregnation concentration and solution. As shown in Table 2, the HCl content of flue gas was added from 15 ppm to 1000 ppm via adjusting the HCl standard gas concentration. The experimental scheme including combustion temperature, air flow rate, addition species, addition method and addition content, was shown in Table 3.

2.3. Simulation methods

In this study, the reaction rate equations were used to calculate and fit the experimental results. The reaction rate equations were inferred via various parameters, including the elementary reaction and reaction equilibrium constant. These parameters were all related to the experimental temperature. These parameters can be converted into the expression form of Arrhenius formula. The reaction rate equations build the relationship with the experimental temperature. Therefore, temperature decrease curve is an important factor for the model fitting. The temperature decrease curve was fitted and calculated via index, logarithm, trigonometric functions and cubic polynomial.

The experimental results were fitted the reaction equations based on the Langmuir-Hinshelwood and Eley-Rideal mechanisms. The parameters in reaction equations was given an initial value and then simulated via the least square method. The various experimental results were continuously fitted via MATLAB until the correlation coefficient (R^2) of two latest fitting results was less than 0.01.

3. Result and discussion

3.1. The influence of Cl addition

The HCl addition and $NaCl/CaCl_2$ impregnation was used to research the Cl influence on the mercury oxidation in Fig. 2. As shown in Fig. 2A, the initial R_{oxy} of sample 01 and sample 02 was about 58–63% and 30–34% without Cl addition, respectively. According to Table S1, the sample 01 had higher fly ash and Cl content as well as lower S, which were all beneficial to the mercury oxidation. Moreover, the SO_2 can suppress the Cl promotion for mercury oxidation as proven in the Figs. S1 and S2. The SO_2 addition decreased the mercury oxidation efficiency.

The HCl addition increased the R_{oxy} in Fig. 2A. When the HCl concentration reached the 400 ppm, the R_{oxy} achieved the highest value. After that, the continued enhancement of HCl concentration did not increased the R_{oxy}. This result could be explained that the adsorption sites of fly ash is limited and the excess HCl could not react with adsorption sites to form the active sites, resulting in gradually tending to the highest R_{oxy}. The similar result was also seen in Fig. 2B. The R_{oxy} gradually rised as the impregnation concentration of NaCl and $CaCl_2$ increased. The R_{oxy} attained the highest value when the impregnation concentration reached 2000 ppm.

The impregnated amount of NaCl and $CaCl_2$ was shifted into the concentration of flue gas. The influence of the three modification methods was compared in Fig. 3. As shown in Fig. 3A, the R_{oxy} of sample 01 reached highest value (77.9%) when the HCl concentration was 400 ppm. The scope of horizontal axis was further shrinked in Fig. 3B. The highest R_{oxy} achieved 75.1% and 82.5% for 40 ppm Cl concentration via adding NaCl and $CaCl_2$, respectively. As shown in Fig. 3C, the highest R_{oxy} of sample 02 was 81.0% when the HCl reached the 600 ppm. In Fig. 3D, the highest R_{oxy} attained 81.9% and 57.4% at the 40 ppm Cl concentration via adding NaCl and $CaCl_2$, respectively. The modification effect for sample 01 followed the order: $CaCl_2 > NaCl > HCl$; the modification effect for sample 02 followed the order: $NaCl > CaCl_2 > HCl$. This proved that both the NaCl and $CaCl_2$ solution impregnation was far more effective than HCl gas addition in same Cl concentration. Previous theoretical calculation studies indicated that the C reacting with the mercury is not the HCl but the Cl*

Table 3
The experimental scheme on the one-dimensional drop furnace.

Coal Sample	T[1] (°C)	Flow Rate[2] (L·min^{-1})	Coal addition (g·h^{-1})	Addition Species	Addition Method	Coal/gas Cl Content(ppm)
01	1100	10	20	–	–	–
02	1100	10	20	–	–	–
01	1100	10	20	NaCl	Impregnation	0–10000
01	1100	10	20	$CaCl_2$	Impregnation	0–10000
01	1100	10	20	HCl	HCl Addition	0–1000
02	1100	10	20	NaCl	Impregnation	0–10000
02	1100	10	20	$CaCl_2$	Impregnation	0–10000
02	1100	10	20	HCl	HCl Addition	0–1000

[1] The T represents the combustion temperature in the furnace.

[2] The Flow Rate represents the flow rate of air through the furnace.

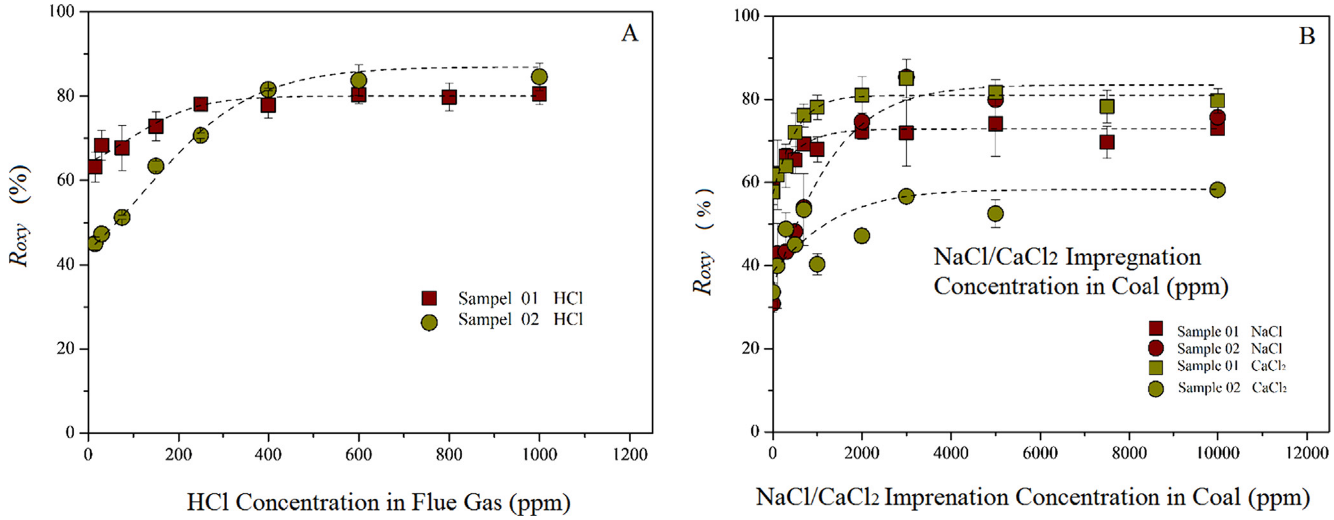

Fig. 2. The influence of Cl addition on the mercury oxidation; A: HCl addition in flue gas; B: NaCl and $CaCl_2$ impregnation concentration of coal.

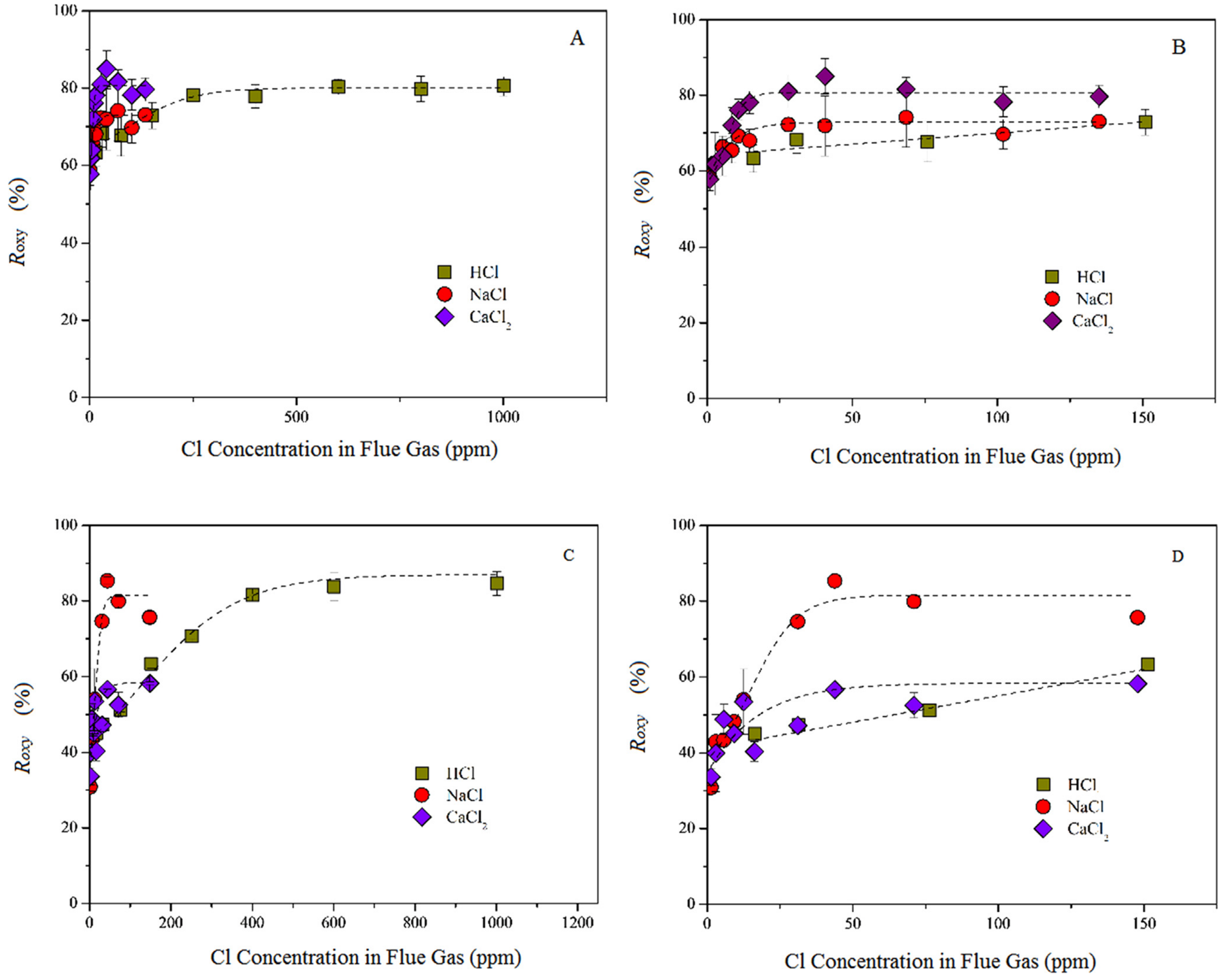

Fig. 3. The comparison of three modification methods (A: Sample 01 (0–1000 ppm); B: Sample 01 (0–150 ppm); C: Sample 02 (0–1000 ppm); D: Sample 02 (0–150 ppm)).

Table 4
The temperature and residence time of different ports.

Testing Port	Residence time (s)	Temperature (°C)
Furnace Outlet	0	1100
0	5.09	373
1	6.78	257
2	7.63	218
3	8.48	195
4	9.33	177
5	10.17	165

in the cooling process of flue gas [35,36]. Therefore, one explanation of the experimental results is that the solution impregnation is easier to form the Cl* than the HCl. Thus, the Cl^{-} in solution could react with carbon atom to form C-Cl groups in the impregnation processing [37,38]. The C-Cl groups was possibly easier to transform into the Cl atom in the combustion processing.

3.2. Heterogeneous mechanism model

Based on the foregoing study, the three modification methods have similar influence regularity. When the Cl concentration reached a certain value, the R_{oxy} did not increase any more. This was ascribed to the amount limitation of active site on the surface of fly ash [39]. The reaction mechanism between the Cl and the mercury follows to the heterogeneous reaction mechanism. The HCl was considered as the key role on the 8 elementary reactions equations (1-1)–(1-8) of mercury oxidation [36,40,41]. Therefore, the heterogeneous reaction of HCl and mercury was fitted and calculated via the E-R and L-H mechanisms.

3.2.1. Eley-Rideal mechanism

The E-R mechanism can be described as follows. The HCl and Hg diffused into the active sites via external and internal diffusion. The HCl reacted with the active site to form transition state HCl (HCl*) which could oxidize the Hg^0 into HgCl*. The HgCl* either desorbs from active site to gas phase in form of HgCl, or reacts with HCl to form the $HgCl_2$*. Then the $HgCl_2$* desorbed to gas phase. So the overall and elementary reactions of E-R mechanism can be described as follows:

Elementary reactions:

$$HCl + {*} \rightarrow HCl^{*} \tag{3-1}$$

$$HCl^{*}+H\ g\rightarrow HgCl^{*} + H \tag{3-2}$$

$$HCl^{*} \rightarrow HCl + {*} \tag{3-3}$$

$$HgCl + HCl^{*} \rightarrow HgCl_2^{*} + H \tag{3-4}$$

$$HCl_2^{*} \rightarrow HgCl_2 + {*} \tag{3-5}$$

Overall reaction:

$$Hg + 2HCl = HgCl_2 + 2H \tag{3-6}$$

Based on foregoing the adsorption and oxidation reaction mechanism between the HCl and the mercury, some hypotheses were made as follows:

(1) The external and internal diffusion had no influence on the experimental result;
(2) The adsorption and desorption of HCl and its transition station was in equilibrium;
(3) The reaction (3-2) and (3-4) was the control step of the reaction rate;
(4) The reaction rate of reaction (3-2) and (3-4) is equal.

Meanwhile, the relative parameters of foregoing reactions were defined as follows:

a. K_1, K_3, K_5 represents the reaction equilibrium constant of reaction (3-1), (3-3) and (3-5), respectively;
b. K_2, K_{-2} represents the forward and reverse reaction rate of reaction (3-2);
c. K_4, K_{-4} represents the forward and reverse reaction rate of reaction (3-4);
d. N_0 represents the amount of available active sites on the surface per unit volume;
e. N_t represents the amount of all active sites on the surface per unit volume;

The overall reaction rate could be described as follows:

$$v = k_2 C_{Hg} C_{HCl*} - k_{-2} C_{HgCl*} C_H = k_4 C_{HgCl} C_{HCl*} - k_{-4} C_{HgCl_2*} C_H \tag{3-7}$$

The equilibrium constant (K_1, K_3, K_5) could be described as follows:

$$K_1 = \frac{C_{HCl*}}{P_{HCl} N_0} \tag{3-8}$$

$$K_3 = \frac{C_{HgCl*}}{C_{HgCl} N_0} \tag{3-9}$$

$$K_5 = \frac{C_{HgCl_2*}}{C_{HgCl_2} N_0} \tag{3-10}$$

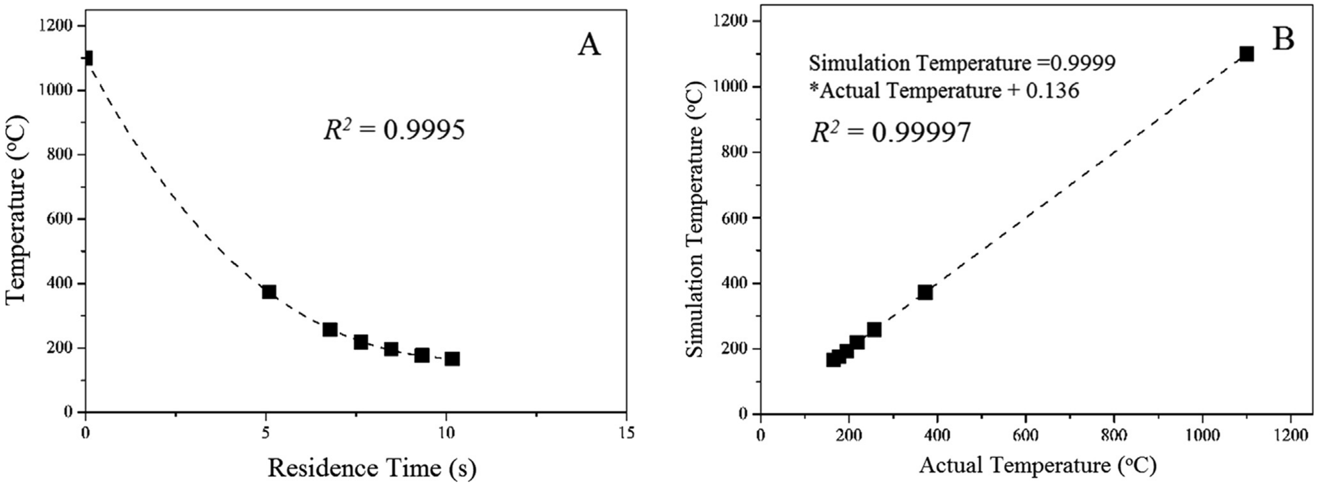

Fig. 4. Fitting result of decreasing temperature of drop furnace (A: temperature and residence time fitting; B: fitting temperature comparison with actual temperature).

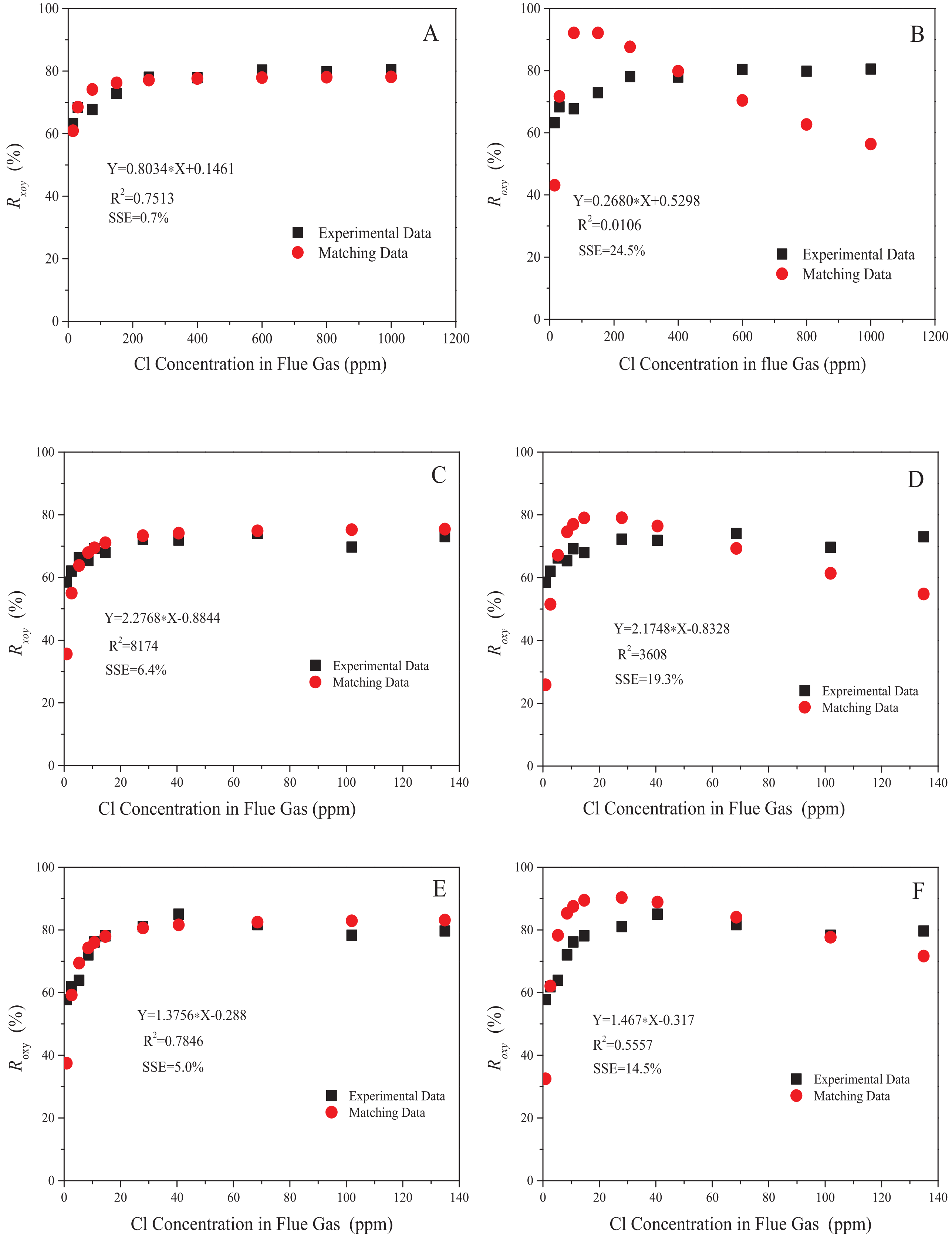

Fig. 5. Fitting result of sample 01 data by the E-R and L-H mechanisms (A, B: HCl addition; C, D: NaCl impregnation; E, F: $CaCl_2$ impregnation; A, C, E: E-R mechanism; B, D, F: L-H mechanism; R^2: correlation coefficient; SSE: sum of squared errors).

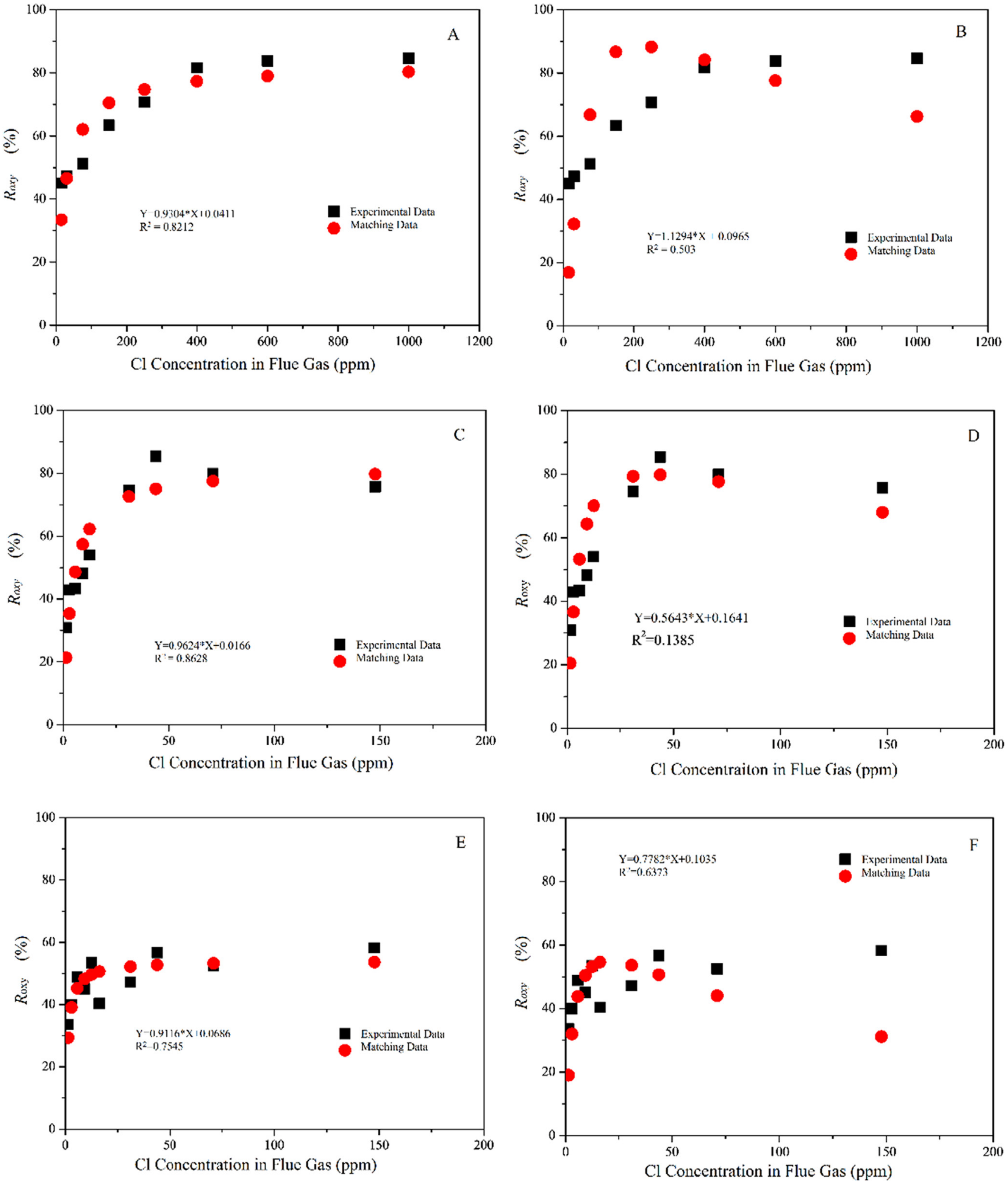

Fig. 6. Fitting result of sample 02 data by the E-R and L-H mechanisms (A, B: HCl addition; C, D: NaCl impregnation; E, F: $CaCl_2$ impregnation; A, C, E: E-R mechanism; B, D, F: L-H mechanism).

where C represents the concentration, such as the C_{HCl*} represents the concentration of the HCl* in the system. P_{HCl} represents the HCl concentration of flue gas.

The amount (N_t) of all active sites on the surface per unit volume was considered to be constant.

$$N_t = N_0 + C_{HCl*} + C_{HgCl*} + C_{HgCl_2*} \tag{3-11}$$

Therefore, the N_0 could be described as follows:

$$N_0 = \frac{N_t}{1 + K_1 P_{HCl} + K_3 C_{HgCl} + K_5 C_{HgCl_2}} \tag{3-12}$$

The overall reaction could be described as follows:

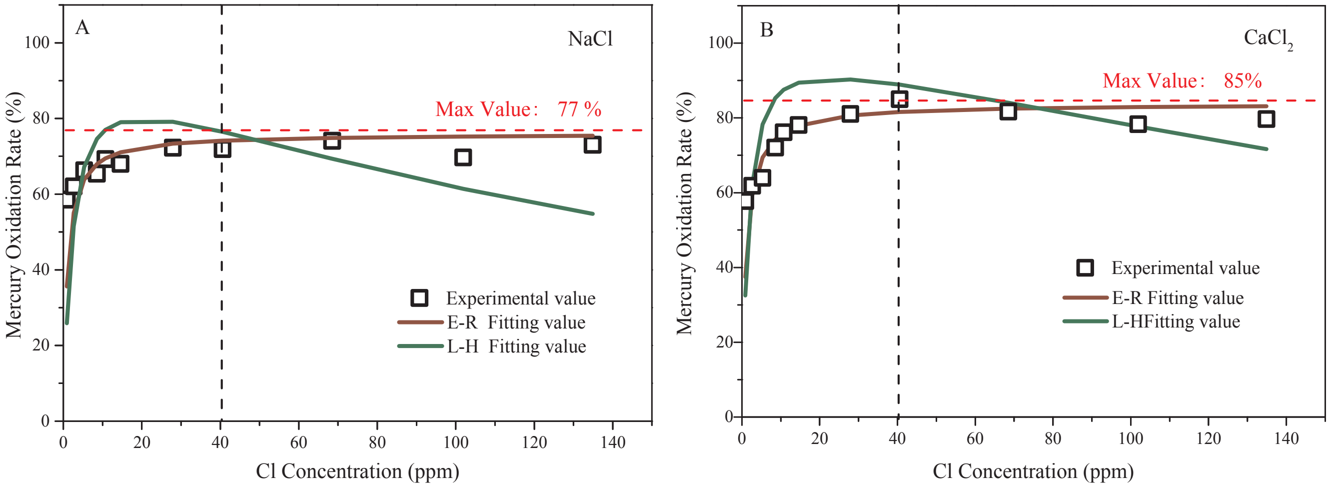

Fig. 7. Fitting comparison of E-R and L-H mechanisms of sample 01 (A: NaCl impregnation; B: $CaCl_2$ impregnation).

$$v = \frac{N_t(k_2K_1P_{HCl}C_{Hg} - k_{-2}K_3C_{HgCl}C_H)}{1 + K_1P_{HCl} + K_3C_{HgCl} + K_5C_{HgCl_2}} \quad (3\text{-}13)$$

Based on the reaction (3-13), this study made following hypotheses: (1) The HCl was the main adsorption substance, yet other substances were difficult to adsorb on the fly ash; (2) The reverse reaction rate of reaction (3-2) was far smaller than the forward reaction rate. Therefore, the reaction (3-13) can be simplified as follows.

$$v = \frac{N_tk_2K_1P_{HCl}C_{Hg}}{1 + K_1P_{HCl}} \quad (3\text{-}14)$$

A new parameter is defined as the$k = N_tk_2K_1$, then the reaction (3-14) can be translated into the reaction (3-15).

$$v = \frac{kP_{HCl}C_{Hg}}{1 + K_1P_{HCl}} \quad (3\text{-}15)$$

3.2.2. *Langmuir-Hinshelwood mechanism*

The L-H mechanism can be described as follows. The HCl and Hg diffused into the active sites via external and internal diffusion. Both HCl and Hg adsorbed on and reacted with the active site to form transition state HCl (HCl*) and mercury (Hg*). The HCl* reacted with Hg* to form the HgCl* on the surface of fly ash. The HgCl* either could desorb from active site to gas phase in form of HgCl, or could react with HCl* to form the $HgCl_2$*. Then the $HgCl_2$* desorbed to gas phase. So the overall and elementary reactions of L-H mechanism can be described as follows:

Elementary reactions:

$$Hg + * \rightarrow Hg^* \quad (3\text{-}16)$$

$$HCl + * \rightarrow HCl^* \quad (3\text{-}17)$$

$$HCl^* + Hg^* \rightarrow HgCl^* + H \quad (3\text{-}18)$$

$$HgCl^* \rightarrow HgCl + * \quad (3\text{-}19)$$

$$HgCl^* + HCl^* \rightarrow HgCl_2^* + H \quad (3\text{-}20)$$

$$HgCl_2^* \rightarrow HgCl_2 + * \quad (3\text{-}21)$$

Overall reaction:

$$Hg + 2HCl = HgCl_2 + 2H \quad (3\text{–}6)$$

The basic hypotheses were same with the E-R mechanism:

(1) The external and internal diffusion had no influence on the experimental result;
(2) The adsorption and desorption of HCl and its transition station was in equilibrium;
(3) The reaction (3-18) and (3-20) was the control step of the reaction rate;
(4) The reaction rate of reaction (3-18) and (3-20) is equal.

Meanwhile, the relative parameters of foregoing reactions was defined as follows:

a. K_1, K_3, K_4 and K_6 represents the reaction equilibrium constant of reaction (3-16), (3-17), (3-19) and (3-21), respectively;
b. K_3, K_{-3} represents the forward and reverse reaction rate of reaction (3-18);
c. K_5, K_{-5} represents the forward and reverse reaction rate of reaction (3-20);
d. N_0 represents the amount of available active sites on the surface per unit volume;
e. N_t represents the amount of all active sites on the surface per unit volume;

The overall reaction rate could be described as follows:

$$v = k_3C_{Hg*}C_{HCl*} - k_{-3}C_{HgCl*} = k_5C_{HgCl*}C_{HCl*} - k_{-5}C_{HgCl_2*} \quad (3\text{-}22)$$

The equilibrium constant (K_1, K_3, K_5) could be described as follows:

$$K_1 = \frac{C_{Hg*}}{P_{Hg}N_0} \quad (3\text{-}23)$$

$$K_2 = \frac{C_{HCl*}}{P_{HCl}N_0} \quad (3\text{-}24)$$

$$K_4 = \frac{C_{HCl*}}{P_{HgCl}N_0} \quad (3\text{-}25)$$

$$K_6 = \frac{C_{HgCl_2*}}{C_{HgCl_2}N_0} \quad (3\text{-}26)$$

where C represents the concentration, such as the C_{HCl^*} represents the concentration of the HCl* in the system. P_{HCl} and P_{Hg} represents the HCl and Hg concentration of flue gas, respectively.

The amount (N_t) of all active sites on the surface per unit volume was considered to be constant.

$$N_t = N_0 + C_{Hg*} + C_{HCl*} + C_{HgCl*} + C_{HgCl_2*} \quad (3\text{-}27)$$

Therefore, the N_0 could be described as follows:

$$N_0 = \frac{N_t}{1 + K_1P_{Hg} + K_2P_{HCl} + K_4C_{HgCl} + K_6C_{HgCl_2}} \quad (3\text{-}28)$$

The overall reaction could be described as follows:

$$v = k_3 C_{Hg*} C_{HCl*} - k_{-3} C_{HgCl*} = k_3 K_1 K_2 P_{Hg} P_{HCl} N_0^2 - k_{-3} K_4 P_{HgCl} N_0 \tag{3-29}$$

$$v = k_3 K_1 K_2 P_{Hg} P_{HCl} N_0^2 - k_{-3} K_4 P_{HgCl} N_0 \tag{3-30}$$

Based on the reaction (3-18) and (3-20), this study made following hypotheses: (1) The C_{HCl^*} approached to zero, namely the product was existed in form of $HgCl_2$; (2) The adsorption ability of $HgCl_2$ was very weak, namely $1 + K_1 P_{Hg} + K_2 P_{HCl} \gg K_6 C_{HgCl2}$.

The reaction rate of overall reaction was simplified as follows:

$$v = \frac{K P_{Hg} P_{HCl}}{(1 + K_1 P_{Hg} + K_2 P_{HCl})^2} \tag{3-31}$$

where $K = N_t^2 k_3 K_1 K_2$.

In conclusion, the reaction rate equations of E-R and L-H mechanisms were inferred to be as follows.

E-R mechanism:

$$v = \frac{k P_{HCl} C_{Hg}}{1 + K_1 P_{HCl}} \tag{3-15}$$

L-H mechanism:

$$v = \frac{K P_{Hg} P_{HCl}}{(1 + K_1 P_{Hg} + K_2 P_{HCl})^2} \tag{3-31}$$

3.2.3. Relation between the temperature and the residence time

The reaction rate equations were inferred via various parameters, including the elementary reaction and reaction equilibrium constant. These parameters were all related to the experimental temperature. These parameters can be converted into the expression form of Arrhenius formula. The reaction rate equations build the relationship with the experimental temperature. In this study, the coal was combusted in 1100 °C and then the Hg^0 was oxidized as the temperature of flue gas decreased. The reaction rate was transformed into be as follows.

$$v = \frac{k P_{HCl} C_{Hg}}{1 + K_1 P_{HCl}} \tag{3-15}$$

where $k = k_0 e^{-E/RT}$, $K = K_1 e^{-E_1/RT}$.

$$v = \frac{K P_{Hg} P_{HCl}}{(1 + K_1 P_{Hg} + K_2 P_{HCl})^2} \tag{3-31}$$

where $K = K_0 e^{-\mathrm{E}/RT}$, $K_1 = K_{10} e^{-\mathrm{E}/RT}$, $K_2 = K_{20} e^{-E_2/RT}$

E-R mechanism:

$$R_{oxy} = \int_0^t vVdt = \int_{T_0}^{T} \frac{vV}{f'(t)} dT = \int_{T_0}^{T} \frac{V}{f'(t)} \frac{K_0 e^{-E/RT} P_{HCl} C_{Hg}}{1 + K_1 e^{-E_1/RT} P_{HCl}} dT \tag{3-32}$$

L-H mechanism:

$$\begin{aligned} R_{oxy} &= \int_0^t vVdt \\ &= \int_{T_0}^{T} \frac{vV}{f'(t)} dT = \int_{T_0}^{T} \frac{V}{f'(t)} \frac{K_0 e^{-E/RT} P_{HCl} P_{Hg}}{1 + K_{10} e^{-E_1/RT} P_{Hg} + K_{10} e^{-E_2/RT} P_{HCl}} dT \end{aligned} \tag{3-33}$$

where the R_{oxy} represents the mercury oxidation efficiency, T represents the temperature of flue gas, t is the residence time.

The finite element method was used to integrated and solved. The component of flue gas on the cross section was uniform and consistent. In the processing of temperature decrease, the residence time was divided into 0.01 s step length and then temperature was calculated at every step length. The differential ($f'(t)$) of the R_{xoi} was calculated at every step length and then integrated to receive the R_{xoi} at the desired temperature. Therefore, the relation between temperature and time was established firstly. The temperature of 0–5 testing ports was measured. The outlet temperature of drop furnace is 1100 °C. The temperature and residence time were listed in Table 4.

The six temperature points were used to fit the temperature of different residence time. Comparing index, logarithm and trigonometric functions, cubic polynomial best fitted the experimental data. The correlation coefficient was 0.99995. The expression equation was shown as follows. The fitting result was shown in Fig. 4.

$$T = 1100.07 - 211.41t + 15.1t^2 - 0.33t^3 \tag{3-34}$$

3.3. Simulation result of Cl addition experiment

The experiment data of three Cl addition methods was fitted and analyzed via simulation methods in Section 2.3. The fitting result was shown in Figs. 5 and 6.

As shown in Fig. 5, the R^2 of E-R and L-H mechanisms for sample 01 had significant difference. The E-R mechanism showed better fitting result than the L-H mechanism. The R^2 of E-R mechanism was 0.7513–0.8174. As the Cl addition increased, both experimental and fitting data increased and then tended to the highest value in E-R mechanism in Fig. 3A, C and E. But the fitting value of L-H mechanism firstly enhanced and then decreased with the Cl addition increasing in Fig. 3B, D and F. This fitting result was not consistent with the experimental data that the excess Cl addition made the R_{oxy} tend to the maximum limit. The R^2 of L-H mechanism was only 0.0106–0.5557. This result indicated that the E-R mechanism was more consistent with the mercury oxidation on the fly ash. Therefore, the amount of active sites on the fly ash was the main limiting factor when the Cl addition is excess. The Cl continuous addition could not form new active sites for the mercury oxidation since the active sites was all occupied. Therefore, the R_{oxy} did not further increase in Fig. 5 when the Cl was excessively added into the flue gas.

The similar fitting result was seen in Fig. 6 as well. The fitting result of E-R mechanism was also far better than that of L-H mechanism. The R^2 of E-R mechanism was in the range of 0.7545–0.8628 while that of L-H mechanism was only 0.1385–0.6373. The downward parabola fitting curve (rose firstly and then descend) of L-H mechanism did not conform to R_{oxy} variation tendency (rose firstly and then tended to highest value).

In order to further contrast the E-R mechanism and the L-H mechanism, the fitting results of sample 01 on the NaCl and $CaCl_2$ were integrated into Fig. 7. The R_{oxy} of sample 01 increased to max value (77% and 85%, respectively) when the Cl addition amount of NaCl and $CaCl_2$ increased to about 40 ppm. Then the R_{oxy} of sample 01 fluctuated in the range of 10%, indicating the Cl active sites reached the saturation adsorption. This result indicated that the promotional influence of Cl addition on the R_{oxy} existed the optimum point. If the addition amount excessed the optimum point, the subsequent Cl addition did not work on the R_{oxy} promotion. As shown in Fig. 7, the fitting result of E-R mechanism well agreed with the experimental data tendence and max value. However, the fitting result of L-H mechanism has obvious difference both in the max R_{oxy} value and the final tendence. The optimum addition amount of L-H mechanism is 15 ppm, which is different from optimum point (40 ppm). The selection of incorrect reaction mechanism possibly results in unsatisfactory promotional effectiveness or the waste of Cl. It implied that the Cl and mercury reaction mechanism conformed to the E-R mechanism. Firstly, the Cl adsorbed on the active sites to form the Cl* groups serving as the mercury oxidation. Then, the Cl* groups directly oxidized the Hg^0 in the gas form into Hg_2Cl_2 or $HgCl_2$. Finally, the $HgCl_2$ transferred from active sites into the flue gas. The active sites could repeatedly react with the Cl to form the Cl* groups.

4. Conclusion

This study used the one-dimensional drop furnace to research the Cl oxidation for the elemental mercury in the flue gas of lignite and subbituminous. Based on the elementary reaction, both E-R and L-H mechanism models were built for the mercury oxidation. The study result found that the increase of Cl concentrations in flue gas has increased the R_{oxy} initially and then tended to the max value via the manner of both HCl gas addition and NaCl/$CaCl_2$ solution impregnation. The NaCl/$CaCl_2$ solution impregnation methods were generally better than the HCl gas addition. This possibly contributed to the C-Cl group formation via the solution impregnation, which was beneficial to the active Cl atom (Cl*) groups formation on the combustion processing. The modification effect followed the order: $CaCl_2$ > NaCl > HCl for lignite and NaCl > $CaCl_2$ > HCl for subbituminous. The coal quality had certain influence on the Cl modification. The high S content suppressed the R_{oxy}. The Cl and Hg^0 oxidation mechanism conformed to the E-R mechanism: the formed Cl* on the active sites directly oxidized the Hg^0 into the Hg_2Cl_2 or $HgCl_2$. Then the Hg_2Cl_2 or $HgCl_2$ transferred from active sites into the gas phase. The promotional influence of three Cl addition methods existed before the optimum point (40 ppm for solution impregnation and 400 ppm for HCl gas addition). If the addition amount excessed the optimum point, the subsequent Cl addition did not work anymore on the R_{oxy} promotion. This result has important guiding significance on the Cl addition method for increasing the Hg^0 oxidation in the future.

Declaration of Competing Interest

The authors declare that they have no known competing financial interests or personal relationships that could have appeared to influence the work reported in this paper.

Acknowledgements

This work was sponsored by National Key Research & Development Plan (2017YFC0210404) and National Natural Science Foundation of China (21625701).

Appendix A. Supplementary data

Supplementary data to this article can be found online at https://doi.org/10.1016/j.fuel.2019.116506.

References

[1] Wu Q, Wang S, Zhang L, Hui M, Wang F, Hao J. Flow analysis of the mercury associated with nonferrous ore concentrates: implications on mercury emissions and recovery in China. Environ Sci Technol 2016;50:1796–803.
[2] Wu Q, Wang S, Li G, Liang S, Lin CJ, Wang Y, et al. Temporal trend and spatial distribution of speciated atmospheric mercury emissions in China during 1978–2014. Environ Sci Technol 2016;50:13428–35.
[3] Hui M, Wu Q, Wang S, Liang S, Zhang L, Wang F, et al. Mercury flows in China and global drivers. Environ Sci Technol 2017;51:222–31.
[4] Frandsen F, Damjohansen K, Rasmussen P. Trace-elements from combustion and gasification of coal – an equilibrium approach. Prog Energy Combust Sci 1994;20:115–38.
[5] Gerasimov GY. Investigation of the behavior of mercury compounds in coal combustion products. J Eng Phys Thermophys 2005;78:668–76.
[6] Senior CL, Sarofim AF, Zeng TF, Helble JJ, Mamani-Paco R. Gas-phase transformations of mercury in coal-fired power plants. Fuel Process Technol 2000;63:197–213.
[7] Sliger R, Going DJ, Kramlich JC. Kinetic investigation of the high-temperature oxidation of mercury by chlorine species. Paper 98F–18, proceedings of western states section/the combustion institute fall 1998 meeting. 1998.
[8] Sliger RN, Kramlich JC, Marinov NM. Towards the development of a chemical kinetic model for the homogeneous oxidation of mercury by chlorine species. Fuel Process Technol 2000;65:423–38.
[9] Edwards JR, Srivastava RK, Kilgroe JD. A study of gas-phase mercury speciation using detailed chemical kinetics. J Air Waste Manage 2001;51:869–77.
[10] Xu MH, Qiao Y, Zheng CG, Li LC, Liu J. Modeling of homogeneous mercury speciation using detailed chemical kinetics. Combust Flame 2003;132:208–18.
[11] Galbreath KC, Zygarlicke CJ. Mercury transformations in coal combustion flue gas. Fuel Process Technol 2000;65:289–310.
[12] Wang S, Zhang L, Zhao B, Meng Y, Hao J. mitigation potential of mercury emissions from coal-fired power plants in China. Energy Fuels 2012;26:4635–42.
[13] Gao Y, Zhang Z, Wu J, Duan L, Umar A, Sun L, et al. A critical review on the heterogeneous catalytic oxidation of elemental mercury in flue gases. Environ Sci Technol 2013;47:10813–23.
[14] Suarez Negreira A, Wilcox J. Uncertainty analysis of the mercury oxidation over a standard SCR catalyst through a lab-scale kinetic study. Energy Fuels 2015;29:369–76.
[15] Li G, Wang S, Wang F, Wu Q, Tang Y, Shen B. Role of inherent active constituents on mercury adsorption capacity of chars from four solid wastes. Chem Eng J 2017;307:544–52.
[16] T.K. Gale, Understanding Mercury Chemistry in Coal-Fired Boilers. Internal Report, Southern Research Institute; 2006.
[17] Benson SA, Holmes MJ, McCollor DP, Mackenzie JM, Crocker CR, Kong L, et al. Large-scale mercury control technology testing for lignite-fired utilities-oxidation systems for wet FGD. University Of North Dakota; 2007.
[18] Wang H, Duan Y, Li Y-N, Xue Y, Liu M. Investigation of mercury emission and its speciation from an oxy-fuel circulating fluidized bed combustor with recycled warm flue gas. Chem Eng J 2016;300:230–5.
[19] Galbreath KC, Zygarlicke CJ, Tibbetts JE, Schulz RL, Dunham GE. Effects of NOx, α-Fe2O3, γ-Fe2O3, and HCl on mercury transformations in a 7-kW coal combustion system. Fuel Process Technol 2005;86:429–48.
[20] Fujiwara N, Fujita Y, Tomura K, Moritomi H, Tuji T, Takasu S, et al. Mercury transformations in the exhausts from lab-scale coal flames. Fuel 2002;81:2045–52.
[21] Pavlish JH, Sondreal EA, Mann MD, Olson ES, Galbreath KC, Laudal DL, et al. Status review of mercury control options for coal-fired power plants. Fuel Process Technol 2003;82:89–165.
[22] Prestbo EM, Bloom NS. Mercury speciation adsorption (Mesa) method for combustion flue-gas – methodology, artifacts, intercomparison, and atmospheric implications. Water Air Soil Pollution 1995;80:145–58.
[23] Wilcox J, Rupp E, Ying SC, Lim D-H, Negreira AS, Kirchofer A, et al. Mercury adsorption and oxidation in coal combustion and gasification processes. Int J Coal Geol 2012;90–91:4–20.
[24] Hall B, Schager P, Lindqvist O. Chemical-reactions of mercury in combustion flue-gases. Water Air Soil Pollut 1991;56:3–14.
[25] Widmer NC, Cole JA, Seeker WR, Gaspar JA. Practical limitation of mercury speciation in simulated municipal waste incinerator flue gas. Combust Sci Technol 1998;134:315–26.
[26] Linak WP, Ryan JV, Ghorishi BS, Wendt JOL. Issues related to solution chemistry in mercury sampling impingers. J Air Waste Manage 2001;51:688–98.
[27] Dunham GE, DeWall RA, Senior CL. Fixed-bed studies of the interactions between mercury and coal combustion fly ash. Fuel Process Technol 2003;82:197–213.
[28] Norton GA, Yang HQ, Brown RC, Laudal DL, Dunham GE, Erjavec J. Heterogeneous oxidation of mercury in simulated post combustion conditions. Fuel 2003;82:107–16.
[29] Presto AA, Granite EJ. Survey of catalysts for oxidation of mercury in flue gas. Environ Sci Technol 2006;40:5601–9.
[30] Hower JC, Senior CL, Suuberg EM, Hurt RH, Wilcox JL, Olson ES. Mercury capture by native fly ash carbons in coal-fired power plants. Prog Energy Combust Sci 2010;36.
[31] Kostova IJ, Hower JC, Mastalerz M, Vassilev SV. Mercury capture by selected Bulgarian fly ashes: influence of coal rank and fly ash carbon pore structure on capture efficiency. Appl Geochem 2011;26:18–27.
[32] Gale TK, Lani BW, Offen GR. Mechanisms governing the fate of mercury in coal-fired power systems. Fuel Process Technol 2008;89:139–51.
[33] Laudal DL, Brown TD, Nott BR. Effects of flue gas constituents on mercury speciation. Fuel Process Technol 2000;65:157–65.
[34] Zhou JS, Luo ZY, Hu CX, Cen KF. Factors impacting gaseous mercury speciation in postcombustion. Energy Fuels 2007;21:491–5.
[35] Niksa S, Fujiwara N, Fujita Y, Tomura K, Moritomi H, Tuji T, et al. A mechanism for mercury oxidation in coal-derived exhausts. J Air Waste Manage 2002;52:894–901.
[36] Wilcox J, Robles J, Marsden DCJ, Blowers P. theoretically predicted rate constants for mercury oxidation by hydrogen chloride in coal combustion flue gases. Environ Sci Technol 2003;37:4199–204.
[37] Li G, Wang S, Wu Q, Wang F, Ding D, Shen B. Mechanism identification of temperature influence on mercury adsorption capacity of different halides modified bio-chars. Chem Eng J 2017;315:251–61.
[38] Li G, Wang S, Wu Q, Wang F, Shen B. Mercury sorption study of halides modified bio-chars derived from cotton straw. Chem Eng J 2016;302:305–13.
[39] Li G, Shen B, Li Y, Zhao B, Wang F, He C, et al. Removal of element mercury by medicine residue derived biochars in presence of various gas compositions. J Hazard Mater 2015;298:162–9.
[40] Niksa S, Fujiwara N. Predicting extents of mercury oxidation in coal-derived flue gases. J Air Waste Manage 2005;55:930–9.
[41] Krishnakumar B, Helble JJ. Understanding mercury transformations in coal-fired power plants: evaluation of homogeneous Hg oxidation mechanisms. Environ Sci Technol 2007;41:7870–5.